JOC The Journal of Organic Chemistry

Article

pubs.acs.org/joc

Nonstatistical Dynamics in the Thermal C^2-C^6/Diels–Alder Cyclization of Enyne-Allenes: Effect of Topology

Debabrata Samanta, Anup Rana, and Michael Schmittel*

Department of Chemistry and Biology, Universität Siegen, Adolf-Reichwein Strasse, D-57068 Siegen, Germany

Supporting Information

ABSTRACT: The thermal C^2-C^6 (Schmittel) cyclization of an enyne-allene with two aryl rings at the allene terminus experimentally leads to three formal Diels–Alder (DA) cycloaddition products, two of which (involving the dimethylamino phenyl unit) are shown to form in a nonstatistical process. DFT computations on the reaction paths reveal that the two aryl rings (Ph vs $PhNMe_2$) do not interact in a dynamic manner as their minimum energy pathways (MEPs) are separated by a large barrier. The preferential formation of the more-hindered DA product **8** (*ortho* to the dimethylamino group) over the less-hindered product **9** (*para* to the dimethylamino group), despite the higher energy TS for **8**, suggests the occurrence of nonstatistical dynamics in the cyclization onto the dimethylamino phenyl unit, though. Potential energy surface (PES) computations indicate that the large amount of nonstatistical dynamics (97%) arises from facile IRC dynamics (left picture) that is compared with the non-IRC dynamics of a related system (~76%, right picture, *J. Org. Chem.* **2014**, 79, 2368).

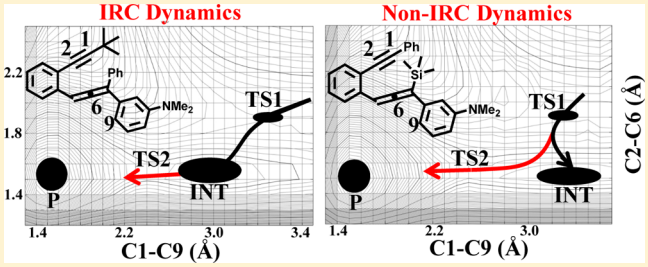

INTRODUCTION

In recent years, the in-depth mechanistic study of long known reaction scenarios has revealed that *nonstatistical dynamics* plays a much more significant role in the thermal reaction of polyatomic molecules than anticipated.[1] Our understanding of the various factors controlling dynamic effects is, however, still underdeveloped. For post-transition-state dynamics, both *excess energy* gathered at the initial TS and used to overcome follow-up barrier(s) and *matching of directionality*, that is, vastly matching vectors of motion along the trajectory, are fundamental requirements.[2] Both elements are crucial to cross the follow-up barrier(s) with *continuation of momentum* prior to intramolecular vibrational energy redistribution (IVR). In addition, Singleton and co-workers have identified dynamic effects on a bifurcating potential energy surface (PES) and revealed that transition state geometry and PES topology are vital parameters to determine selectivity.[3] However, experimental evidence on these scenarios is very scarce. A key problem is the difficulty to experimentally recognize and quantify dynamic effects.[4,5] At present, the amount of nonstatistical dynamics is mostly computed by costly dynamic trajectory calculations on simplified structural models,[1a,6] by the weak collision Rice-Ramsperger-Kassel-Marcus (RRKM)/master equation model[7] or, alternatively, by the canonical competitive nonstatistical model (CCNM).[8] The two later models, though, are not only tedious and never used on larger molecules, in addition, they have not yet been sufficiently validated.

Recently, we have developed a straightforward assay based on simple DFT computations and experimental results to estimate the amount of nonstatistical dynamics in the thermal C^2-C^6 (Schmittel)[9,10]/Diels–Alder cyclization of enyne-allenes **1a–c** (Scheme 1).[5] With **1a–c** exhibiting a similar directionality of the minimum energy path, that is, surface topology, we were able to validate the hypothesis of excess energy as a decisive factor controlling the amount of nonstatistical dynamics. In detail, we located two initial high-energy C^2-C^6 TSs, **1-TS1**$_O^{‡}$ and **1-TS1**$_P^{‡}$, which connect enyne-allene **1** to the σ,π-diradical intermediate **1-INT** by the minimum energy path (MEP). The shallow well at intermediate **1-INT** opens two low-energy exit channels toward the cyclization products **1-CP**$_O$ and **1-CP**$_P$ via the two TSs **1-TS2**$_O^{‡}$ and **1-TS2**$_P^{‡}$, respectively. Notably, occurrence of nonstatistical dynamics in the reaction mechanism is indicated because the more hindered product **2** forms in excess amount over **3**.

Intriguingly, the observed product ratios **2**:**3** very closely match the statistical partitioning created at the two initial TSs **1-TS1**$_O^{‡}$ and **1-TS1**$_P^{‡}$, suggesting that after crossing these high-energy TSs the molecules use the collected momentum to move directly toward the products. Indeed, a careful assessment revealed an MEP at the initial TSs with a straight directionality toward the products. The subsequent MEP, however, departs from this shortest route to the products by following a bent trail to the intermediate thus sacrificing the required directionality for nonstatistical dynamics. Using a simple algorithm, we calculated that 71–86% of the reacting molecules did follow the non-IRC dynamical path, and notably, this amount increased with augmenting energy difference between initial and follow-up TSs.

Received: November 26, 2014
Published: February 3, 2015

DOI: 10.1021/jo502693b
J. Org. Chem. 2015, 80, 2174–2181

Scheme 1. C^2-C^6/Diels-Alder Reaction of Enyne-Allenes[a]

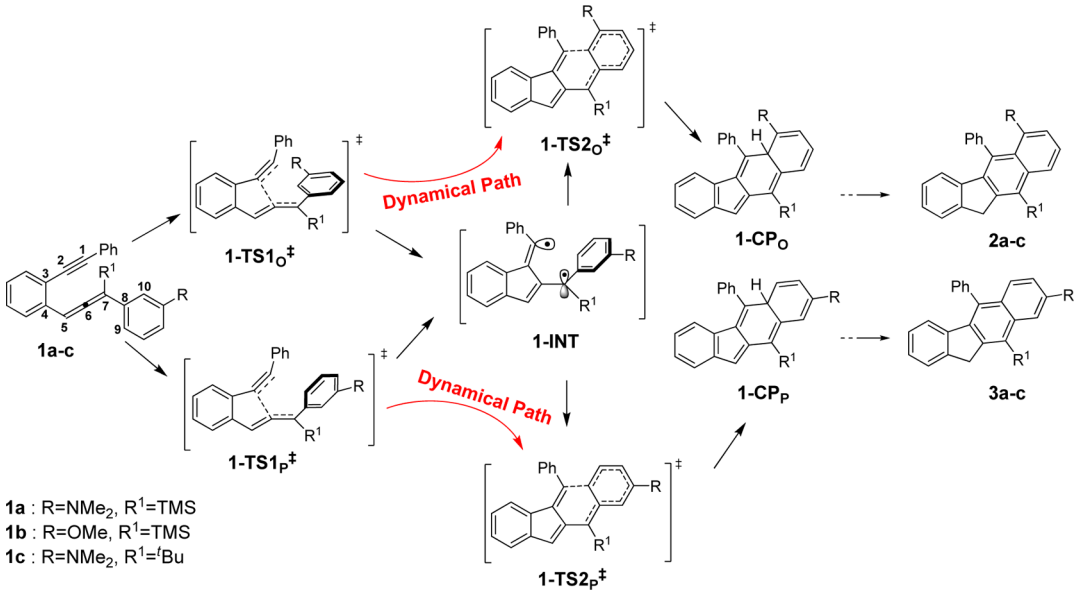

[a]**TS1** and **TS2** represent the initial and follow-up TSs, respectively, while the subscripts **O** and **P** describe the conformation (proximity of reactive alkynyl unit toward the *ortho* or *para* position of PhR) or the final connectivity in the cyclization product **CP**.

The focus of the present paper is to vary the directionality of the MEP by modifying the substituents at the enyne-allene and to analyze the resulting effect on the amount of post-TS nonstatistical dynamics.

RESULTS AND DISCUSSION

In order to perturb the directionality of MEP, we introduced a second phenyl ring at the allene terminus, see enyne-allene **7** (Scheme 2), while the 3-*N*,*N*-dimethylaminophenyl unit was maintained at the allene terminus to experimentally probe the regioselectivity. A *t*-butyl group was placed at the alkyne terminus to produce an enyne-allene that is thermally stable at room temperature.

Scheme 2. Synthesis of Enyne-Allene 7

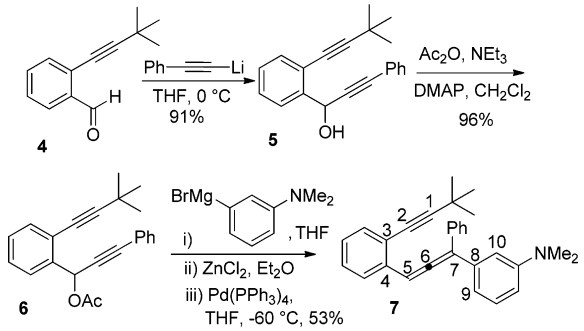

Enyne-allene **7** was prepared in a three-step synthesis from 2-(3,3-dimethylbut-1-ynyl)benzaldehyde (**4**) by first adding phenylethynyllithium, followed by acetylation of the resultant propargyl alcohol **5** with acetic anhydride in the presence of catalytic amounts of DMAP. Formation of **7** was finalized by introducing the probing aryl group via a palladium catalyzed zincate addition (with arylmagnesium bromide, $ZnCl_2$ and $Pd(PPh_3)_4$). All compounds were fully characterized using IR, ^1H-, ^{13}C-, and $^1H-^1H$ COSY NMR spectroscopy, and elemental analysis.

When enyne-allene **7** was thermolyzed in dry and degassed toluene, the constitutionally isomeric compounds **8**–**10** were obtained as thermolysis products (Scheme 3). After their separation by long-bed flash column chromatography, they were fully characterized by IR, ^1H, ^{13}C, and $^1H-^1H$ COSY NMR spectroscopy, and elemental analysis. Markedly, in **8**, the strong steric repulsion between the *t*-butyl and *N*,*N*-dimethylamino groups creates a distorted naphthyl ring,[11] rendering the two fulvenyl protons diastereotopic, as indicated by a geminal coupling ^2J = 22.0 Hz in the ^1H NMR.[12]

For evaluation of the temperature effect on product selectivity, the thermolysis was performed in the range from 60 to 140 °C (sealed tube) maintaining partial conversion. The product ratios were determined by analyzing the ^1H NMR spectrum of the crude reaction mixture. A continuous decrease in product

Scheme 3. Thermolysis of Enyne-Allene 7

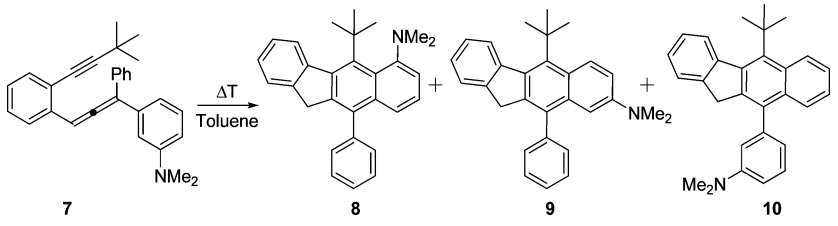

DOI: 10.1021/jo502693b
J. Org. Chem. 2015, 80, 2174–2181

Table 1. Experimental Product Ratios of 8, 9, and 10 in the Thermolysis of Enyne-Allene 7[a]

temp. (°C)	time (min)	ratio[b] **10:9:8**	temp. (°C)	time (min)	ratio[b] **2a/3a**
	7			**1a**	
60	360	2.40:1:1.42	60	180	1.65:1
80	180	2.24:1:1.40	70	75	1.62:1
100	60	2.21:1:1.37	80	70	1.60:1
120	30	2.15:1:1.34	90	50	1.58:1
140	15	2.12:1:1.32	100	40	1.56:1

[a]Thermolysis data of **1a**, taken from ref 8, are added for comparison. [b]Obtained from the crude ^{1}H NMR spectra. Standard deviation of ratios = ±0.01−0.03.

selectivity of **8**:**9** was observed with increasing temperature from 60 to 140 °C (Table 1). At first, the temperature dependence of this product ratio seems to be a convincing argument not to consider the occurrence of nonstatistical dynamics, but the privileged formation of the more hindered product **8** points to the involvement of nonstatistical dynamics in the reaction mechanism. On the other side, selectivity between the two aryl groups at the allene terminus is poor (phenyl vs *m*-*N*,*N*-dimethylaminophenyl substitution ≈ 1:1.1) over the whole temperature range. The thermolysis of **1a** also showed a similar decrease of product ratio at the *m*-*N*,*N*-dimethylaminophenyl unit with increasing temperature.[5]

By comparing various DFT methods in regard to accuracy for the Bergman and Myers-Saito cyclizations, Schreiner et al.[13] suggested to apply the pure DFT functionals in correlation with Lee, Yang, and Parr as the most suitable methods with a 6-31G(d) basis set. Therefore, we utilized the (BS)-UBLYP/6-31G(d)[14] method, as implemented in *Gaussian 09*, to optimize all stationary points and transition states. For comparison, we computed the free energy values at 25 °C. A thermochemical analysis at different temperatures revealed that the free energy differences between TSs discussed herein did not change significantly within the experimental temperature range.

Despite ample efforts, we were unable to locate concerted TSs; rather, each trial resulted in the identification of a C^2-C^6 TS. The outcome of the DFT computations and statistical predictions may be summarized as follows (Figure 1): the cyclization reaction involving the $PhNMe_2$ ring in enyne-allene **7** proceeds in a stepwise fashion via the formation of the σ,π-diradical intermediates **7-INT$_O$** or **7-INT$_P$**, with the initial TSs (C^2-C^6) being higher in energy than the follow-up TSs. The initial TSs (C^2-C^6), **7-TS1$_O$**‡ and **7-TS1$_P$**‡, which connect the enyne-allene **7** to intermediates **7-INT$_O$** and **7-INT$_P$** via the MEP, were located at 21.57 and 21.85 kcal mol^{-1}, respectively.

Two follow-up TSs, **7-TS2$_O$**‡ (19.38 kcal mol^{-1}) and **7-TS2$_P$**‡ (17.90 kcal mol^{-1}), link the intermediates **7-INT$_O$** and **7-INT$_P$** to the products **7-CP$_O$** (more-hindered) and **7-CP$_P$** (less-hindered), respectively. A transition state **7-TS$_{OP}$**‡, responsible for the rotational interconversion between **7-INT$_O$** and **7-INT$_P$**, was located at 18.33 kcal mol^{-1}. Because **7-TS2$_O$**‡ is higher in energy than **7-TS$_{OP}$**‡ and **7-TS2$_P$**‡ by 1.05 and 1.48 kcal mol^{-1}, respectively, one would expect a 9.35 times preferential formation of **9** (from less hindered product **7-CP$_P$**) over **8** (from more hindered product **7-CP$_O$**) at 60 °C. However, the experimentally observed preference is reversed (**8**:**9** = 1.42:1 at 60 °C)! Interestingly, with **7-TS1$_O$**‡ being lower in energy than **7-TS1$_P$**‡ by 0.28 kcal mol^{-1}, the statistical partitioning created at the two initial TSs is 1.53:1 at 60 °C, which is very close to the experimentally observed product ratio 1.42:1. Such coincidence corroborates our suggestion for the occurrence of nonstatistical dynamics in the reaction.

Potential energy surfaces (PES, Figure 2a,b) were computed with 351 points (0.1 Å × 0.1 Å) by varying the C2−C6 and C1−C9 or C1−C10 distances, which are principal reaction coordinates for the Diels−Alder reaction. As stated earlier, no separate saddle point for a concerted TS could be identified on any of the surfaces. Rather, the PESs show a broad region about the saddle of **7-TS1$_P$**‡ (Figure 2a) and **7-TS1$_O$**‡ (Figure 2b), with no concerted character as clearly visible from the very long C1−C9 (3.60 Å in **7-TS1$_P$**‡) and C1−C10 (3.59 Å in **7-TS1$_O$**‡) distances. Free energy surfaces were also computed by

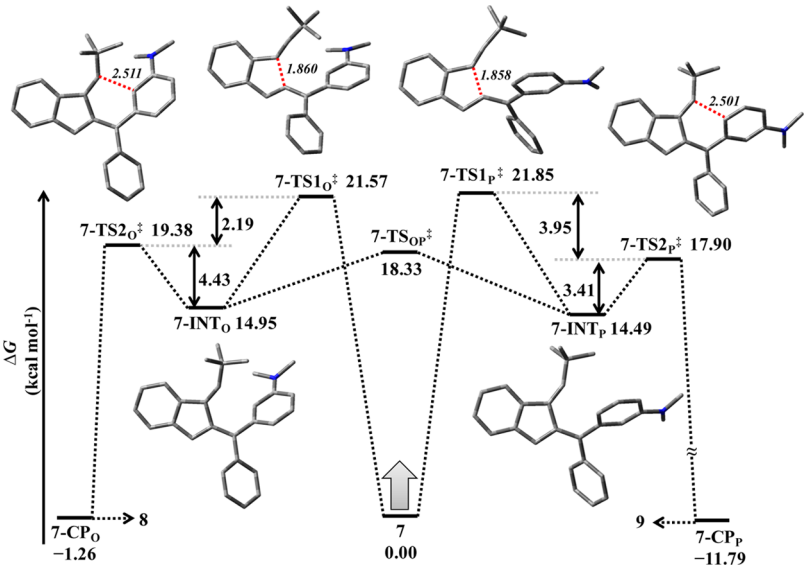

Figure 1. Reaction profile for the thermal cyclization of **7**, affording **8** and **9**, as determined at (BS)-UBLYP/6-31G(d) level. Free energies (kcal mol^{-1} at 25 °C) are reported with reference to the reactive conformer of enyne-allene **7** (ΔG = 0). Distances are shown in Å (italics). Hydrogen atoms are omitted for clarity.

DOI: 10.1021/jo502693b
J. Org. Chem. 2015, 80, 2174−2181

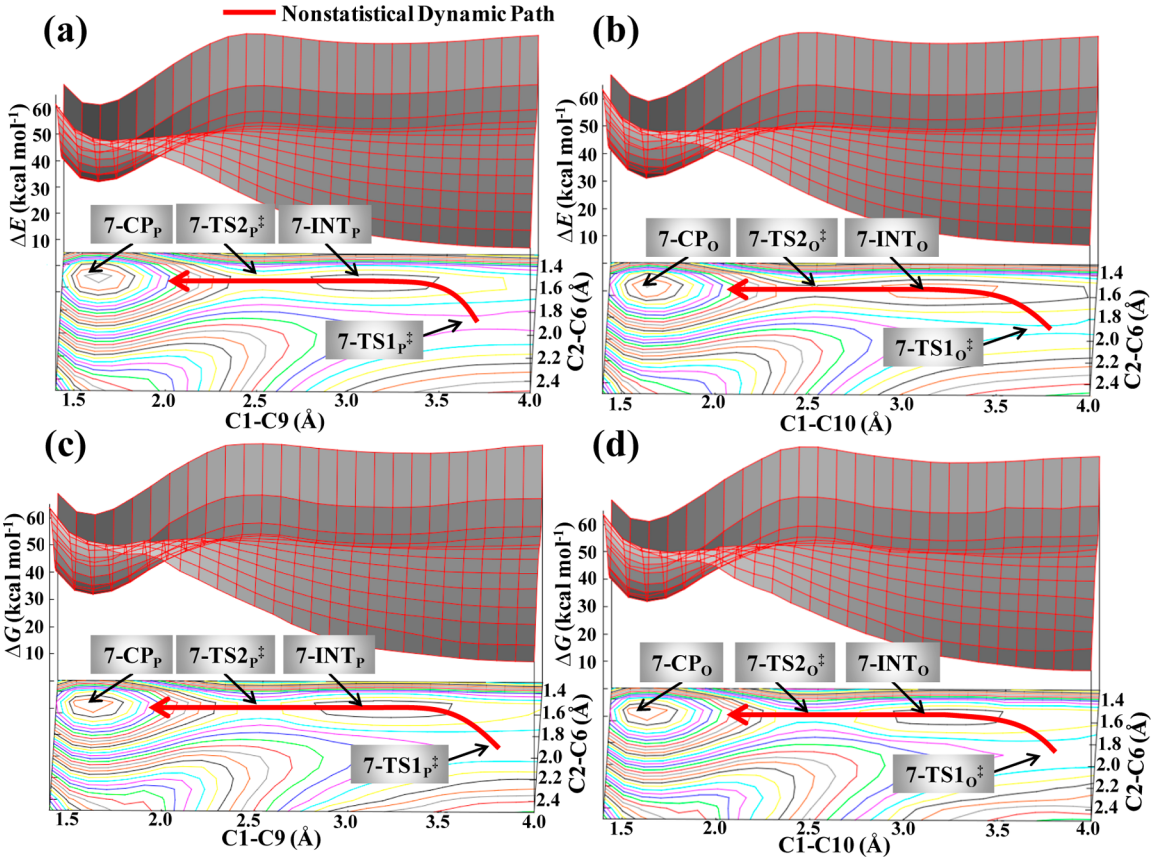

Figure 2. 3D potential energy surfaces (a, b) and free energy surfaces at 25 °C (c, d) were computed by scanning the C2−C6 distance from 2.5 to 1.3 Å and the C1−C9 or C1−C10 distance from 1.4 to 4.0 Å (0.1 Å × 0.1 Å grid size) using (BS)-UBLYP/6-31G(d).

Table 2. Comparison of the Amount of Nonstatistical Dynamics (ND) Calculated on the Basis of Three Different Functionals, That Is, (BS)-UBLYP, (BS)-UOLYP, and (BS)-UG96LYP[a]

method	temp (°C)	$\Delta G^{\ddagger}_{\text{1a-TS1}_P}{}^{\ddagger} - \Delta G^{\ddagger}_{\text{1a-TS1}_O}{}^{\ddagger}$ (Q_1)	$\Delta G^{\ddagger}_{\text{1a-TS2}_O}{}^{\ddagger} - \Delta G^{\ddagger}_{\text{1a-TS2}_P}{}^{\ddagger}$ (Q_2)	ND_{1a} (%)	$\Delta G^{\ddagger}_{\text{7-TS1}_P}{}^{\ddagger} - \Delta G^{\ddagger}_{\text{7-TS1}_O}{}^{\ddagger}$ (Q_1)	$\Delta G^{\ddagger}_{\text{7-TS2}_O}{}^{\ddagger} - \Delta G^{\ddagger}_{\text{7-TS2}_P}{}^{\ddagger}$ (Q_2)	ND_7 (%)	$ND_7 - ND_{1a}$ (%)
(BS)-UBLYP/ 6-31G(d)	60	0.77 (3.23:1)	1.06 (1:4.99)	76	0.28 (1.53:1)	1.48 (1:9.35)	96	20
	80	0.77 (3.02:1)	1.06 (1:4.55)	76	0.28 (1.49:1)	1.48 (1:8.24)	97	21
	100	0.77 (2.85:1)	1.06 (1:4.20)	76	0.28 (1.46:1)	1.48 (1:7.36)	97	21
(BS)-UOLYP/ 6-31G(d)	60	0.63 (2.59:1)	1.25 (1:6.61)	83	0.29 (1.55:1)	1.87 (1:16.8)	96	13
	80	0.63 (2.45:1)	1.25 (1:5.94)	83	0.29 (1.51:1)	1.87 (1:14.4)	96	13
	100	0.63 (2.34:1)	1.25 (1:5.40)	83	0.29 (1.48:1)	1.87 (1:12.4)	96	13
(BS)-UG96LYP/ 6-31G(d)	60	0.64 (2.63:1)	1.62 (1:11.5)	84	0.25 (1.46:1)	1.70 (1:13.0)	99	15
	80	0.64 (2.49:1)	1.62 (1:10.1)	84	0.25 (1.43:1)	1.70 (1:11.3)	99	15
	100	0.64 (2.37:1)	1.62 (1:8.89)	84	0.25 (1.40:1)	1.70 (1:9.90)	99	15

[a]Computed free energy differences are reported in kcal mol^{-1}, from which the partitioning Q_1 or Q_2 at the different TS (in parentheses) was derived using the Eyring equation. ND is calculated using the algorithm[15] $X_{ns}Q_1 + X_sQ_2 = Q_{exp}$ for which experimental data (Q_{exp}) is taken from Table 1. $ND_7 - ND_{1a}$ indicates the enhancement of ND from **1a** to **7**. Data related to **1a** with (BS)-UBLYP/6-31G(d) method were taken from ref 8 and are presented for comparison.

thermochemical analysis of all optimized structures on the PESs and, notably, here the broadening around these saddles increased (Figure 2c,d).

Both the potential and free energy surfaces show that the initial TS (C^2−C^6), diradical intermediate, and follow-up TS are aligned along one direction. Therefore, under dynamic conditions, molecules crossing the initial TSs, **7-TS1$_O$**‡ or **7-TS1$_P$**‡, will directly proceed to the product **7-CP$_O$** or **7-CP$_P$**. However, not all reacting molecules will follow a nonstatistical dynamical path, as a certain fraction should relax in the intermediate well. The relaxed molecules will statistically partition to produce both **7-CP$_O$** and **7-CP$_P$** according to the two follow-up TSs **7-TS2$_O$**‡ and **7-TS2$_P$**‡. To estimate the amount of nonstatistical dynamics, we utilized the same algorithm $X_{ns}Q_1 + X_sQ_2 = Q_{exp}$ as earlier for **1a** (Table 2).[15] Accordingly, in the reaction of enyne-allene **7**, 97% of the reacting molecules that cross **7-TS1$_O$**‡ and **7-TS1$_P$**‡ overcome the follow-up barriers in a dynamic fashion, while in the closely related enyne-allenes **1**, this fraction is slightly lower at 71−86%.

In our earlier paper, the excess energy guiding the amount of nonstatistical dynamics was approximated from the energy difference between the initial and follow-up TS(s). In **1a** and **7**,

DOI: 10.1021/jo502693b
J. Org. Chem. 2015, 80, 2174−2181

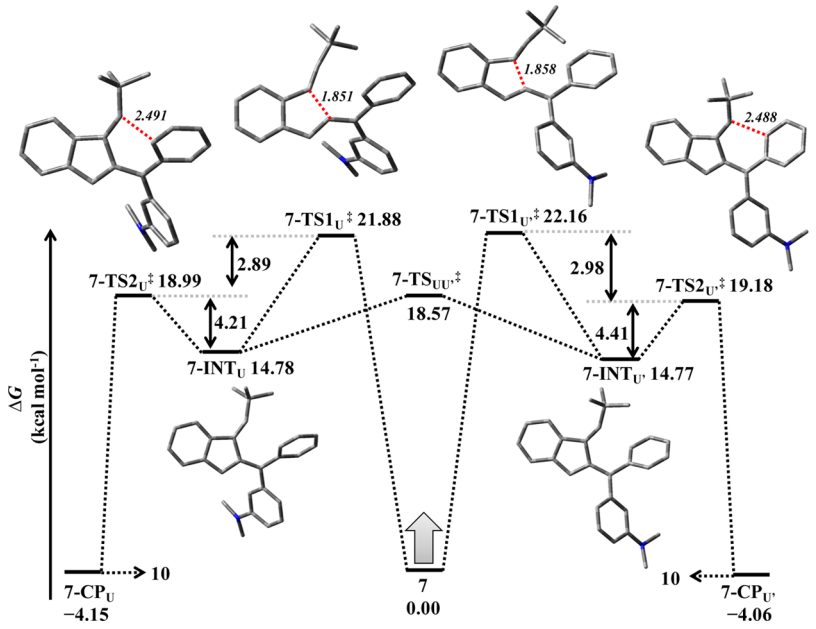

Figure 3. Reaction profile for the thermal cyclization of **7** producing **10** at (BS)-UBLYP/6-31G(d) level. Free energies are reported at 25 °C. Distances are shown in angstrom unit (italics). The subscripts U and U′ (representing two slightly different conformations) denote the reaction channel involving the unsubstituted phenyl ring. Hydrogens are omitted for clarity.

Table 3. Optimized Free Energy Values for the Initial TSs, 7-TS1$_O$‡, 7-TS1$_P$‡, 7-TS1$_U$‡, and 7-TS1$_{U'}$‡, Obtained Using (BS)-UBLYP/6-31G(d), (BS)-UOLYP/6-31G(d), and (BS)-UG96LYP/6-31G(d) Methods (in kcal mol^{-1} at 100 °C)[a]

methods	7-TS1$_O$‡	7-TS1$_P$‡	7-TS1$_U$‡	7-TS1$_{U'}$‡	(8 + 9):10
(BS)-UBLYP/6-31G(d)	21.57	21.85	21.88	22.16	1.52:1
(BS)-UOLYP/6-31G(d)	21.48	21.78	21.67	21.94	1.27:1
(BS)-UG96LYP/6-31G(d)	22.19	22.43	22.43	22.26	1.06:1

[a]The ratio (**8** + **9**):**10** in the right most column was derived from the partitioning created at the initial TSs (**7-TS1$_O$**‡, **7-TS1$_P$**‡, **7-TS1$_U$**‡, and **7-TS1$_{U'}$**‡) using Eyring equation.

these energy differences are −2.94 (**1a-TS1$_O$**‡ → **1a-TS2$_O$**‡), −4.77 (**1a-TS1$_P$**‡ → **1a-TS2$_P$**‡), −2.19 (**7-TS1$_O$**‡ → **7-TS2$_O$**‡), and −3.95 (**7-TS1$_P$**‡ → **7-TS2$_P$**‡) kcal mol^{-1}, respectively, revealing surprisingly that **7** should be a less dynamically controlled system than **1**.

Such contradiction needs a closer inspection. A notable difference between **1a** and **7** is the directionality of the MEP. In enyne-allene **1a**, the C1−C9 distance changes along the MEP from 3.35 → 3.41 (increase) → 2.55 Å (decrease) when going from the initial TS (**1a-TS1$_P$**‡) → intermediate (**1a-INT**) → follow-up TS (**1a-TS2$_P$**‡), indicating that conservation of momentum is not possible following MEP. Thus, the cyclization behavior was explained by postulating that enyne-allene **1** follows a non-IRC dynamics. In contrast, in enyne-allene **7**, the C1−C9 distance along the MEP changes from 3.60 → 3.15 → 2.50 Å when going from **7-TS1$_P$**‡ → **7-INT$_P$** → **7-TS2$_P$**‡, indicating a facile continuation of momentum. Similarly, a continuous decreases of C1−C10 distance was also observed on the MEP after crossing **7-TS1$_O$**‡. The potential and free energy surfaces (Figure 2) also show that stationary points are aligned in one direction, and thus, all molecules should overcome the follow-up barrier, preferably with a direct continuation of momentum supporting nonstatistical behavior.

The free energy difference between **7-TS1$_O$**‡ and **7-TS1$_P$**‡ is only 0.28 kcal mol^{-1} at (BS)-UBLYP, which is very delicate as the percentage of nonstatistical dynamics depends greatly on it. In order to verify consistency of the computational results, we additionally optimized the initial and follow-up TSs for **1a** and **7** with other DFT methods. The predicted energy differences between **7-TS1$_O$**‡ and **7-TS1$_P$**‡ are 0.29 and 0.25 kcal mol^{-1} at (BS)-UOLYP and (BS)-G96LYP level, respectively, providing consistent results. In contrast, the free energy differences between **1a-TS1$_O$**‡ and **1a-TS1$_P$**‡ (two C^2−C^6 TSs for **1a**) are 0.77, 0.63, and 0.64 kcal mol^{-1} with (BS)-UBLYP, (BS)-UOLYP and (BS)-UG96LYP methods, respectively, showing a slight variation. Importantly, with all the applied methods, there is an increase of the nonstatistical dynamics in going from **1a** to **7** in the order of 13−21% (Table 2).

Similar to the reaction involving the PhNMe$_2$ ring in enyne-allene **7**, we also located two separate C^2−C^6 TSs, **7-TS$_U$**‡ and **7-TS$_{U'}$**‡, for the reaction onto the Ph ring, depending on the two possible orientations of the nonreacting PhNMe$_2$ ring that convert **7** to **7-INT$_U$** and **7-INT$_{U'}$**, respectively (Figure 3). The barrier for interconverting (**7-TS$_{OU}$**‡) the two intermediates, **7-INT$_O$** and **7-INT$_U$**, was located at 19.68 kcal mol^{-1} with the (BS)-UBLYP method. Because this barrier is higher in energy than that of all follow-up TSs, the reaction paths leading to formation of **10** do not interact with those leading to **8** and **9**, and the product ratio (between two aryl rings PhNMe$_2$ and Ph) can be calculated from the initial (C^2−C^6) TS energies (Table 3). For instance, at 100 °C, the selectivity between the two aryl rings, PhNMe$_2$/Ph, is predicted to be 1.52:1, 1.27:1, and 1.06:1 using (BS)-UBLYP, (BS)-UOLYP, and (BS)-G96LYP methods,

DOI: 10.1021/jo502693b
J. Org. Chem. 2015, 80, 2174−2181

respectively, in rather good agreement with the experiment (1.07:1).

In summary, we present a system, in which molecules mostly comply with nonstatistical dynamics. The amount of nonstatistical dynamics varies depending on the directionality of MEP, that is, whether the MEP allows for a continuation of momentum. The enhancement of nonstatistical dynamics in **7** points to the fundamental necessity of directional motion for dynamics.

EXPERIMENTAL SECTION

General Methods. Anhydrous solvents were used to perform reactions under inert atmosphere (argon). Diethyl ether (Et_2O) was predried over calcium hydride and then distilled over sodium. Potassium was utilized to dry tetrahydrofuran (THF) and toluene. Triethylamine (Et_3N) and dichloromethane (DCM) were dried over calcium hydride. All compounds were purified by flash column chromatography (silica gel, 0.035−0.070 mm). To describe NMR signals, the following abbreviations were utilized: s = singlet, d = doublet, t = triplet, td = triplet of doublets, dd = doublet of doublets, ddd = doublet of doublets of doublets, m = multiplet. For numbering the molecular carbon skeletons in the NMR assignments, we did not follow IUPAC nomenclature rules. 2-(3,3-Dimethylbut-1-ynyl)benzaldehyde (**4**) was prepared according to the reported procedure.[16]

*Synthesis of 1-(2-(3,3-Dimethylbut-1-ynyl)phenyl)-3-phenylprop-2-yn-1-ol (**5**).* 2.5 M *n*-BuLi in hexane (9.66 mL, 24.2 mmol) was added

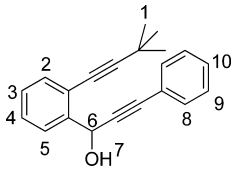

dropwise to a stirred solution of phenylacetylene (2.66 mL, 24.2 mmol) in 50 mL of dry THF at 0 °C under inert atmosphere. After stirring the reaction mixture for 30 min, a solution of 2-(3,3-dimethylbut-1-ynyl)benzaldehyde (**4**; 3.00 g, 16.1 mmol) in 20 mL of dry THF was added. The resulting solution was then allowed to warm to room temperature and stirred for 3 h. It was quenched with water and extracted three times with ethyl acetate. The combined organic layer was concentrated and the crude product was purified by flash column chromatography (*n*-hexane/ethyl acetate = 98:2, R_f = 0.35) over silica gel. Yellow oil: 91% yield (4.23 g, 14.7 mmol). IR (KBr): $\tilde{\nu}$ 3395, 3063, 2968, 2869, 2233, 1598, 1483, 1450, 1366, 1291, 1203, 1101, 1031, 961, 918, 822, 758 cm^{-1}; ^1H NMR (400 MHz, CD_2Cl_2) δ 1.36 (s, 9H, 1-H), 2.92 (d, ^3J = 6.2 Hz, 1H, 7-H), 6.00 (d, ^3J = 6.2 Hz, 1H, 6-H), 7.29 (td, ^3J = 7.4 Hz, ^4J = 1.4 Hz, 1H, 3-H), 7.32−7.38 (m, 4H, 4, 9, 10-H), 7.43 (dd, ^3J = 7.4 Hz, ^4J = 1.6 Hz, 1H, 2-H), 7.45−7.49 (m, 2H, 8-H), 7.69 (dd, ^3J = 7.7 Hz, ^4J = 1.4 Hz, 1H, 5-H) ppm; ^{13}C NMR (100 MHz, CD_2Cl_2) δ 28.5, 30.9, 64.0, 76.7, 86.1, 88.9, 105.0, 122.3, 122.9, 126.7, 128.4 (2C), 128.7, 128.8, 131.9, 132.6, 142.6 ppm; Anal. Calcd for $C_{21}H_{20}O$: C, 87.46; H, 6.99. Found: C, 87.07; H, 6.94.

*Synthesis of 1-(2-(3,3-Dimethylbut-1-ynyl)phenyl)-3-phenylprop-2-ynyl Acetate (**6**).* A total of 0.790 mL of acetic anhydride (8.32 mmol)

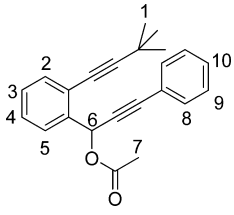

was added dropwise to a stirred solution of 1-(2-(3,3-dimethylbut-1-ynyl)phenyl)-3-phenylprop-2-yn-1-ol (**5**; 2.18 g, 7.57 mmol), 4-dimethylaminopyridine (184 mg, 1.51 mmol), and 3 mL of dry triethylamine in 100 mL of dry dichloromethane at 0 °C. After stirring for 1 h, the reaction mixture was washed with water (3 × 50 mL). The organic layer was separated, concentrated at reduced pressure, and purified by flash column chromatography (*n*-hexane/ethyl acetate (98:2), R_f = 0.52); colorless oil: 96% yield (2.40 g, 7.27 mmol). IR (KBr): $\tilde{\nu}$ 3062, 2968, 2868, 2359, 2231, 1744, 1486, 1449, 1367, 1335, 1220, 1016, 954, 915, 757 cm^{-1}; ^1H NMR (400 MHz, C_6D_6) δ 1.30 (s, 9H, 1-H), 1.68 (s, 3H, 7-H), 6.85−6.93 (m, 4H, 3, 9, 10-H), 7.03 (td, ^3J = 7.6 Hz, ^4J = 1.2 Hz, 1H, 4-H), 7.34−7.36 (m, 2H, 8-H), 7.41 (dd, ^3J = 7.6 Hz, ^4J = 1.2 Hz, 1H, 2-H), 7.63 (s, 1H, 6-H), 8.02 (dd, ^3J = 7.6 Hz, ^4J = 1.2 Hz, 1H, 5-H) ppm; ^{13}C NMR (100 MHz, C_6D_6) δ 20.4, 28.4, 30.9, 64.7, 76.9, 86.7, 87.3, 104.8, 122.8, 124.3, 128.1, 128.5, 128.5, 128.8, 129.0, 132.2, 132.5, 139.1, 169.1 ppm; Anal. Calcd for $C_{23}H_{22}O_2$: C, 83.60; H, 6.71. Found: C, 83.68; H, 6.71.

*Synthesis of 3-(3-(2-(3,3-Dimethylbut-1-ynyl)phenyl)-1-phenylpropa-1,2-dienyl)-N,N-dimethylaniline (**7**).* Under argon atmosphere,

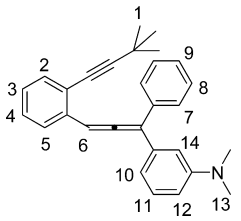

(3-(dimethylamino)phenyl)magnesium bromide (12.1 mmol) in dry THF (25 mL) was added dropwise to a solution of $ZnCl_2$ (1.15 g, 8.47 mmol) in dry diethyl ether (40 mL) at room temperature. After stirring the reaction mixture for 30 min, it was cooled to −60 °C and $Pd(PPh_3)_4$ (350 mg, 303 μmol) in dry THF (20 mL) was added. Subsequently, the reaction mixture was stirred for 15 min at the same temperature. A solution of propargyl acetate **6** (1.00 g, 3.03 mmol) in dry THF (30 mL) was added dropwise. The reaction mixture was allowed to warm up to room temperature. After stirring for 12 h, it was quenched with a saturated ammonium chloride solution and extracted with diethyl ether (3 × 50 mL). The combined organic layers were dried over Na_2SO_4 and concentrated. Purification of the crude product was performed by flash column chromatography over silica gel (*n*-hexane/diethyl ether (98:2), R_f = 0.24; yellow oil): 53% yield (628 mg, 1.60 mmol). IR (KBr): $\tilde{\nu}$ 3058, 3025, 2967, 2869, 2803, 2232, 1927, 1596, 1492, 1445, 1353, 1295, 1227, 1177, 1064, 998, 952, 919, 833, 760 cm^{-1}; ^1H NMR (400 MHz, CD_2Cl_2) δ 1.38 (s, 9H, 1-H), 2.92 (s, 6H, 13-H), 6.72 (ddd, ^3J = 8.1 Hz, ^4J = 2.2 Hz, ^4J = 0.4 Hz, 1H, 12-H), 6.76 (d, ^3J = 7.8 Hz, 1H, 10-H), 6.81 (d, ^4J = 2.2 Hz, 1H, 14-H), 7.16 (td, ^3J = 7.6 Hz, ^4J = 1.2 Hz, 1H, 3-H), 7.21−7.25 (m, 2H, 4, 11-H), 7.28 (s, 1H, 6-H), 7.30 (tt, ^3J = 7.2 Hz, ^4J = 1.4 Hz, 1H, 9-H), 7.34−7.38 (m, 2H, 8-H), 7.41 (dd, ^3J = 7.6 Hz, ^4J = 1.3 Hz, 1H, 2-H), 7.44−7.47 (m, 2H, 7-H), 7.59 (dd, ^3J = 7.9 Hz, ^4J = 1.2 Hz, 1H, 5-H) ppm; ^{13}C NMR (100 MHz, CD_2Cl_2) δ 28.5, 31.1, 40.7, 77.4, 95.8, 104.2, 112.3, 112.9, 114.6, 117.2, 122.4, 126.5, 127.2, 127.8, 128.1, 128.7, 128.7, 129.4, 132.7, 135.4, 136.7, 137.0, 151.3, 209.1 ppm; Anal. Calcd for $C_{29}H_{29}N$: C, 88.96; H, 7.47; N, 3.58. Found: C, 89.17; H, 7.55; N, 3.64.

*Thermolysis of 3-(3-(2-(3,3-Dimethylbut-1-ynyl)phenyl)-1-phenylpropa-1,2-dienyl)-N,N-dimethylaniline (**7**) Producing Compounds **8**, **9**, and **10**.* A solution of 250 mg (638 μmol) of enyne-allene **7** in dry and degassed toluene (25 mL) was taken in a sealed tube and heated for 2 h at 120 °C. Subsequently, the solution was concentrated under reduced pressure, and the constitutionally isomeric products were separated by flash column chromatography over silica gel using 1% diethyl ether in pentane as eluent.

*5-tert-Butyl-N,N-dimethyl-10-phenyl-11H-benzo[b]fluoren-6-amine (**8**).* R_f = 0.23; semisolid compound, 21% yield (134 μmol, 52.0 mg). IR (KBr): $\tilde{\nu}$ 3028, 2926, 2864, 2825, 2781, 1597, 1546, 1478, 1389, 1305, 1185, 1046, 994, 950, 920, 754, 707 cm^{-1}; ^1H NMR (400 MHz, CD_2Cl_2) δ 1.66 (s, 9H, 1-H), 2.43 (s, 3H, 14 or 15-H), 2.86 (s, 3H, 15 or 14-H), 3.73 (d, ^2J = 22.0 Hz, 1H, 6 or 7-H), 3.82 (d, ^2J = 22.0 Hz, 1H, 7 or 6-H), 7.00 (dd, ^3J = 7.2 Hz, ^4J = 1.3 Hz, 1H, 13-H), 7.10 (dd, ^3J = 8.1 Hz, ^4J = 1.3 Hz, 1H, 11-H), 7.16 (dd, ^3J = 8.1 Hz, ^3J = 7.2 Hz, 1H, 12-H), 7.25 (td, ^3J = 7.4 Hz, ^4J = 1.0 Hz, 1H, 4-H), 7.37−7.44 (m, 4H, 3, 5, 9-H), 7.45−7.47 (m, 1H, 10-H), 7.51−7.56 (m, 2H, 8-H), 8.32 (d, ^3J = 8.0 Hz,

DOI: 10.1021/jo502693b
J. Org. Chem. 2015, 80, 2174−2181

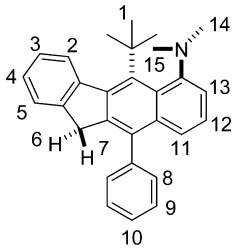

1H, 2-H) ppm; ^{13}C NMR (100 MHz, CD_2Cl_2) δ 32.5, 37.2, 39.5, 41.7, 47.9, 113.3, 120.1, 124.7, 125.0, 126.2, 126.5, 127.3, 127.9, 128.7, 128.8, 130.1, 130.4, 130.8, 132.5, 134.3, 140.0, 140.4, 140.6, 144.2, 144.5, 145.1, 153.2 ppm (due to the distortion within the naphthyl unit, the rotation of the phenyl ring is slow on the NMR time scale producing six ^{13}C signals); Anal. Calcd for $C_{29}H_{29}N$: C, 88.96; H, 7.47; N, 3.58. Found: C, 88.84; H, 7.51; N, 3.56.

*5-tert-Butyl-N,N-dimethyl-10-phenyl-11H-benzo[b]fluoren-8-amine (**9**).* R_f = 0.17; white solid, mp =91 °C, 14% yield (89.0 μmol, 35.0

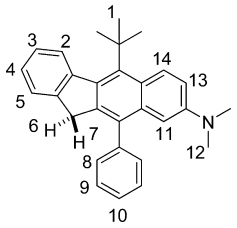

mg). IR (KBr): $\tilde{\nu}$ 3058, 2960, 2913, 2797, 1614, 1504, 1403, 1340, 1161, 1126, 1061, 1025, 985, 946, 812, 779, 715 cm^{-1}; ^{1}H NMR (400 MHz, CD_2Cl_2) δ 1.86 (s, 9H, 1-H), 2.86 (s, 6H, 12-H), 3.74 (s, 2H, 6, 7-H), 6.55 (d, ^4J = 2.8 Hz, 1H, 11-H), 7.02 (dd, ^3J = 9.6 Hz, ^4J = 2.8 Hz, 1H, 13-H), 7.19 (td, ^3J = 7.7 Hz, ^4J = 1.0 Hz, 1H, 4-H), 7.32 (td, ^3J = 7.7 Hz, ^4J = 1.2 Hz, 1H, 3-H), 7.37−7.40 (m, 3H, 5, 9-H), 7.44 (tt, ^3J = 7.2 Hz, ^4J = 1.2 Hz, 1H, 10-H), 7.51−7.56 (m, 2H, 8-H), 8.04 (d, ^3J = 7.7 Hz, 1H, 2-H), 8.34 (d, ^3J = 9.6 Hz, 1H, 14-H) ppm; ^{13}C NMR (100 MHz, CD_2Cl_2) δ 33.3, 37.5, 37.9, 40.5, 104.6, 112.6, 124.8, 125.7, 125.8, 126.6, 127.2, 128.4, 128.9 (2C), 130.3, 131.7, 134.6, 135.8, 140.4, 141.4, 143.4, 144.0, 144.3, 147.5 ppm; Anal. Calcd for $C_{29}H_{29}N$: C, 88.96; H, 7.47; N, 3.58. Found: C, 89.13; H, 7.69; N, 3.58.

*3-(5-tert-Butyl-11H-benzo[b]fluoren-10-yl)-N,N-dimethylaniline (**10**).* R_f = 0.19; white solid, mp = 144 °C, 43% yield (274 μmol, 107 mg).

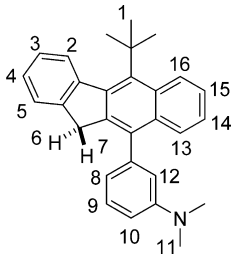

IR (KBr): $\tilde{\nu}$ 3062, 2961, 2920, 2802, 1596, 1494, 1432, 1357, 1225, 1178, 1148, 1059, 994, 952, 858, 763, 709 cm^{-1}; ^{1}H NMR (400 MHz, CD_2Cl_2) δ 1.87 (s, 9H, 1-H), 2.97 (s, 6H, 11-H), 3.82 (d, ^2J = 22.0 Hz, 1H, 6 or 7-H), 3.89 (d, ^2J = 22.0 Hz, 1H, 7 or 6-H), 6.69−6.73 (m, 2H, 8, 12-H), 6.84 (ddd, ^3J = 8.4 Hz, ^4J = 2.6 Hz, ^4J = 0.7 Hz, 1H, 10-H), 7.23−7.29 (m, 2H, 4, 14-H), 7.32−7.40 (m, 3H, 3, 9, 15-H), 7.44 (d, ^3J = 7.4 Hz, 1H, 5-H), 7.58 (dd, ^3J = 8.4 Hz, ^4J = 1.3 Hz, 1H, 13-H), 8.09 (d, ^3J = 8.0 Hz, 1H, 2-H), 8.44 (dd, ^3J = 8.7 Hz, ^4J = 0.5 Hz, 1H, 16-H) ppm; ^{13}C NMR (100 MHz, CD_2Cl_2) δ 33.3, 37.4, 38.0, 40.7, 111.5, 114.3, 118.3, 122.4, 124.3, 125.0, 125.8, 126.0, 126.7, 127.3, 128.9, 129.5, 132.9, 133.5, 134.1, 139.1, 140.3, 140.7, 142.7, 143.7, 144.8, 151.3 ppm; Anal. Calcd for $C_{29}H_{29}N$: C, 88.96; H, 7.47; N, 3.58. Found: C, 88.66; H, 7.50; N, 3.54.

■ ASSOCIATED CONTENT

Supporting Information

Synthesis, spectroscopic, and computational data. This material is available free of charge via the Internet at http://pubs.acs.org.

■ AUTHOR INFORMATION

Corresponding Author

*E-mail: schmittel@chemie.uni-siegen.de.

Notes

The authors declare no competing financial interest.

■ ACKNOWLEDGMENTS

We are indebted to the Deutsche Forschungsgemeinschaft (Schm 647/18-1) for financial support and to Prof. Ralph Jaquet (Universität Siegen) for helpful support concerning the computational infrastructure. We are thankful to the University of Siegen for providing the High-Performance-Computing (HPC) Linux Cluster HorUS for computations.

■ REFERENCES

(1) (a) Kless, A.; Nendel, M.; Wilsey, S.; Houk, K. N. *J. Am. Chem. Soc.* **1999**, *121*, 4524. (b) Oyola, Y.; Singleton, D. A. *J. Am. Chem. Soc.* **2009**, *131*, 3130. (c) Wang, Z.; Hirschi, J. S.; Singleton, D. A. *Angew. Chem., Int. Ed.* **2009**, *48*, 9156. (d) Xu, L.; Doubleday, C. E.; Houk, K. N. *J. Am. Chem. Soc.* **2010**, *132*, 3029. (e) Alder, R. W.; Harvey, J. N.; Lloyd-Jones, G. C.; Oliva, J. M. *J. Am. Chem. Soc.* **2010**, *132*, 8325. (f) Quijano, L. M. M.; Singleton, D. A. *J. Am. Chem. Soc.* **2011**, *133*, 13824. (g) Herath, N.; Suits, A. G. *J. Phys. Chem. Lett.* **2011**, *2*, 642. (h) Gonzalez-James, O. M.; Kwan, E. E.; Singleton, D. A. *J. Am. Chem. Soc.* **2012**, *134*, 1914. (i) Lan, Y.; Danheiser, R. L.; Houk, K. N. *J. Org. Chem.* **2012**, *77*, 1533. (j) Samanta, D.; Cinar, M. E.; Das, K.; Schmittel, M. *J. Org. Chem.* **2013**, *78*, 1451. (k) Samanta, D.; Rana, A.; Schmittel, M. *J. Org. Chem.* **2014**, *79*, 8435. (l) Biswas, B.; Collins, S. C.; Singleton, D. A. *J. Am. Chem. Soc.* **2014**, *136*, 3740. (m) Chen, Z.; Nieves-Quinones, Y.; Waas, J. R.; Singleton, D. A. *J. Am. Chem. Soc.* **2014**, *136*, 13122.

(2) (a) Carpenter, B. K. *Acc. Chem. Res.* **1992**, *25*, 520. (b) Carpenter, B. K. *Angew. Chem.* **1998**, *110*, 3532. (c) Carpenter, B. K. *Chem. Soc. Rev.* **2006**, *35*, 736. (d) Ess, D. H.; Wheeler, S. E.; Iafe, R. G.; Xu, L.; Çelebi-Ölçüm, N.; Houk, K. N. *Angew. Chem., Int. Ed.* **2008**, *47*, 7592. (e) Carpenter, B. K. *Chem. Rev.* **2013**, *113*, 7265.

(3) (a) Thomas, J. B.; Waas, J. R.; Harmata, M.; Singleton, D. A. *J. Am. Chem. Soc.* **2008**, *130*, 14544. (b) Quijano, L. M. M.; Singleton, D. A. *J. Am. Chem. Soc.* **2011**, *133*, 13824.

(4) Schmittel, M.; Vavilala, C.; Jaquet, R. *Angew. Chem., Int. Ed.* **2007**, *46*, 6911.

(5) Samanta, D.; Rana, A.; Schmittel, M. *J. Org. Chem.* **2014**, *79*, 2368.

(6) (a) Rehbein, J.; Carpenter, B. K. *Phys. Chem. Chem. Phys.* **2011**, *13*, 20906. (b) Siebert, M. R.; Zhang, J.; Addepalli, S. V.; Tantillo, D. J.; Hase, W. L. *J. Am. Chem. Soc.* **2011**, *133*, 8335. (c) Black, K.; Liu, P.; Xu, L.; Doubleday, C.; Houk, K. N. *Proc. Natl. Acad. Sci. U.S.A.* **2012**, *109*, 12860.

(7) Glowacki, D. R.; Liang, C. H.; Marsden, S. P.; Harvey, J. N.; Pilling, M. J. *J. Am. Chem. Soc.* **2010**, *132*, 13621.

(8) Zheng, J.; Papajak, E.; Truhlar, D. G. *J. Am. Chem. Soc.* **2009**, *131*, 15754.

(9) (a) Schmittel, M.; Strittmatter, M.; Kiau, S. *Tetrahedron Lett.* **1995**, *36*, 4975. (b) Schmittel, M.; Kiau, S.; Siebert, T.; Strittmatter, M. *Tetrahedron Lett.* **1996**, *37*, 7691. (c) Schmittel, M.; Maywald, M.; Strittmatter, M. *Synlett* **1997**, 165. (d) Cinar, M. E.; Vavilala, C.; Fan, J.; Schmittel, M. *Org. Biomol. Chem.* **2011**, *9*, 3776. (e) Schmittel, M.; Vavilala, C.; Cinar, M. E. *J. Phys. Org. Chem.* **2012**, *25*, 182. (f) Cinar, M. E.; Vavilala, C.; Jaquet, R.; Bats, J. W.; Schmittel, M. *Eur. J. Org. Chem.* **2014**, 5166.

(10) Kraka, E.; Cremer, D. *WIREs Comput. Mol. Sci.* **2014**, *4*, 285−324 DOI: 10.1002/wcms.1174.

DOI: 10.1021/jo502693b
J. Org. Chem. 2015, 80, 2174−2181

(11) Yamamoto, K.; Oyamada, N.; Xia, S.; Kobayashi, Y.; Yamaguchi, M.; Maeda, H.; Nishihara, H.; Uchimaru, T.; Kwon, E. *J. Am. Chem. Soc.* **2013**, *135*, 16526.
(12) Pople, J. A.; Bothner-By, A. A. *J. Chem. Phys.* **1965**, *42*, 1339.
(13) Prall, M.; Wittkopp, A.; Schreiner, P. R. *J. Phys. Chem. A* **2001**, *105*, 9265.
(14) (a) Lee, C.; Yang, W.; Parr, R. G. *Phys. Rev. B* **1988**, *37*, 785. (b) Becke, A. D. *Phys. Rev. A* **1988**, *38*, 3098.
(15) The fraction of dynamically reacting molecules was calculated as following: $X_{ns}Q_1 + X_sQ_2 = Q_{exp}$, where $X_{ns} + X_s = 1$, X_{ns} = mole fraction of molecules following the nonstatistical (ns) dynamically controlled pathway; X_s = mole fraction of molecules following the statistically (s) controlled pathway; Q_1 = partitioning created at the initial (C^2–C^6) TSs; Q_2 = partitioning created at the second TSs; and Q_{exp} = experimental product ratio. Due to the low amount of X_s, no correction was made for the competitive interconversion of both intermediates at the second TS.
(16) Schmittel, M.; Kiau, S.; Siebert, T.; Strittmatter, M. *Tetrahedron Lett.* **1996**, *37*, 7691.

DOI: 10.1021/jo502693b
J. Org. Chem. 2015, 80, 2174–2181